JOURNAL OF GEOPHYSICAL RESEARCH, VOL. 105, NO. D22, PAGES 26,931–26,945, NOVEMBER 27, 2000

The episodic nature of air pollution transport from Asia to North America

James J. Yienger,[1] Meredith Galanter,[2] Tracey A. Holloway,[3] Mahesh J. Phadnis,[1] Sarath K. Guttikunda,[1] Gregory R. Carmichael,[1] Walter J. Moxim,[4] and Hiram Levy II[4]

Abstract. We employ the Geophysical Fluid Dynamics Laboratory (GFDL) global chemistry transport model (GCTM) to address the episodic nature of trans-Pacific pollution. The strongest Asian CO episodes over North America (NA), occurring most frequently between February and May, are often associated with disturbances that entrain pollution over eastern Asia and amplify over the western Pacific Ocean. Using 55 ppb of Asian CO as a criterion for major events, we find that during a typical year three to five Asian pollution events analogous to those observed by *Jaffe et al.* [1999] are expected in the boundary layer all along the U.S. West Coast between February and May. In contrast to CO, Asia currently has a small impact on the magnitude and variability of background ozone arriving over NA from the west. Direct and indirect Asian contributions to episodic O_3 events over the western United States are generally in the 3 - 10 ppbv range. The two largest total O_3 events (>60 ppbv), while having trajectories which pass over Asia, show negligible impact from Asian emissions. However, this may change. A future emission scenario in which Asian NO_x emissions increase by a factor of 4 from those in 1990 produces late spring ozone episodes at the surface of California with Asian contributions reaching 40 ppb. Such episodic contributions are certain to exacerbate local NA pollution events, especially in elevated areas more frequently exposed to free tropospheric and more heavily Asian - influenced air.

1. Introduction

Long-range transport of aerosols and trace gases from Asia significantly alters the composition of the remote Pacific troposphere [e.g., *Uematsu et al.*, 1983; *Merrill et al.*, 1985; *Levy and Moxim*, 1989; *Xiao et al.*, 1997; *Brasseur et al.*, 1996; *Jaffe et al.*, 1997]. In spring, when storm and frontal activity in Asia is most prevalent, seasonally maximum outflows of continental pollution and dust are observed in both in situ observations and satellite studies [*Duce et al.*, 1980; *Bodhaine et al.*, 1981; *Prospero*, 1985; *Prospero and Savoie*, 1989; *Merrill et al.*, 1989; *Herman et al.*, 1997; *Stegmann and Tindale*, 1999], and it has been speculated that the springtime ozone maximum at Hawaii may be caused in large part by Asian air pollution [*Ridley et al.*, 1997; *Wang et al.*, 1998].

There is growing observational evidence for an Asian impact extending to North America. *Kritz* [1990] found evidence that Asian boundary layer air can be transported to the upper troposphere over California in 2-4 days. More recently, *Jaffe et al.* [1999] observed Asian air pollution being transported to the surface of North America (NA) during the spring of 1997. The following year, a visible plume of dust from a strong April Asian dust storm was carried over North America (R. B. Husar, The Asian dust event of April 1998, http://capita.wustl.edu/Asia-FarEast), and *Jaffe et al.* [2000] has again detected Asian pollution off of Washington State in the spring of 1999.

Three-dimensional (3-D) global chemical transport models (GCTMs) are also being used to study the issue. Employing a coarse resolution (8°x10°) GCTM, *Berntsen et al.* [1996] concluded that future developments in Asia will significantly perturb free tropospheric ozone chemistry and, more recently, found that Asian emissions raised average simulated background springtime levels of CO and O_3 by an average of 34 and 4 ppbv, respectively, over the eastern North Pacific [*Berntsen et al.*, 1999]. *Jacob et al.* [1999] recently concluded that rising Asian emissions may generate enough surface background ozone over the western United States to counteract gains from domestic control strategies.

While the previous simulations provide an estimation of the monthly or seasonal mean enhancements, observations suggest that Asian outflow is highly episodic [e.g., *Atlas et al.*, 1992] and may not be well represented as a uniform "background" enhancement. *Berntsen et al.* [1999] simulated episodic trans-Pacific pollution events over NA in their GCTM study, but they found modest low-frequency fluctuations in total CO and day-to-day fluctuations in the Asian CO signal of only a few parts per billion per day. In reality, synoptic-scale fluctuations are much stronger with concentrations of CO at Cheeka Peak Observatory (CPO) changing over a few days by 20 to 50 ppb [*Jaffe et al.*, 2000]. At the peak of one episode at CPO, hydrocarbon levels approached those typically found offshore of Asia during the Pacific Exploratory Mission (PEM) West B mission [see *Jaffe et al.*, 1999 Table 2].

For our examination of the episodic nature of trans-Pacific pollution, we employ the Geophysical Fluid Dynamics

[1]Center for Global and Regional Environmental Research, University of Iowa, Iowa City.
[2]Department of Geosciences, Princeton University, Princeton, New Jersey.
[3]Atmospheric and Oceanic Sciences Program, Princeton University, Princeton, New Jersey.
[4]NOAA Geophysical Fluid Dynamics Laboratory, Princeton, New Jersey.

Paper number 2000JD900309.
0148-0227/00/2000JD900309$09.00

Laboratory (GFDL) global chemistry transport model (GCTM), which has sufficient resolution to produce synoptic-scale tracer fluctuations similar in magnitude and nature to those observed in the real atmosphere [see *Levy and Moxim*, 1989; *Moxim*, 1990; *Moxim et al.*, 1996]. We address questions such as how well is the Asian pollution signal over North America represented by a mean value? How frequent are strong transport events (i.e., like those observed by *Jaffe et al.* [1999] at CPO) expected during and outside of spring, and how does this frequency differ with location and altitude? What is the relationship between elevated O_3 levels over NA and Asian emissions?

2. Model Description

2.1. GCTM

The GCTM has a horizontal resolution of ~265 km (2.4° x 2.4° in the tropics and 3°-3.5° x 2.4° in midlatitudes) and 11 sigma levels in the vertical at standard pressures of 10, 38, 65, 110, 190, 315, 500, 685, 835, 940, and 990 mbar and is driven by 1 year of 6-hour time-averaged winds, 6-hour sampled temperatures, and 6-hour summed precipitation fields from a general circulation model with no diurnal cycle [*Manabe et al.*, 1974]. Resolved transport is solved to second order in the horizontal and fourth order in the vertical [see *Mahlman and Moxim*, 1978 section 3], and diffusion-based parameterizations for horizontal sub-grid scale transport and for vertical sub-grid-scale transport due to dry and moist convection throughout the troposphere and shear-dependent mixing in the boundary layer are included [see *Levy et al.*, 1985; *Kasibhatla et al.*, 1996] see also the appendix of *Levy et al.* [1999] and references therein for details.

In Figure 1 we see that the GCTM's North Pacific wind fields averaged over March and April are quite reasonable and in good agreement with climatology. The primary features throughout the troposphere of both are a high-latitude cyclonic circulation over eastern Siberia in the upper troposphere and its associated lower

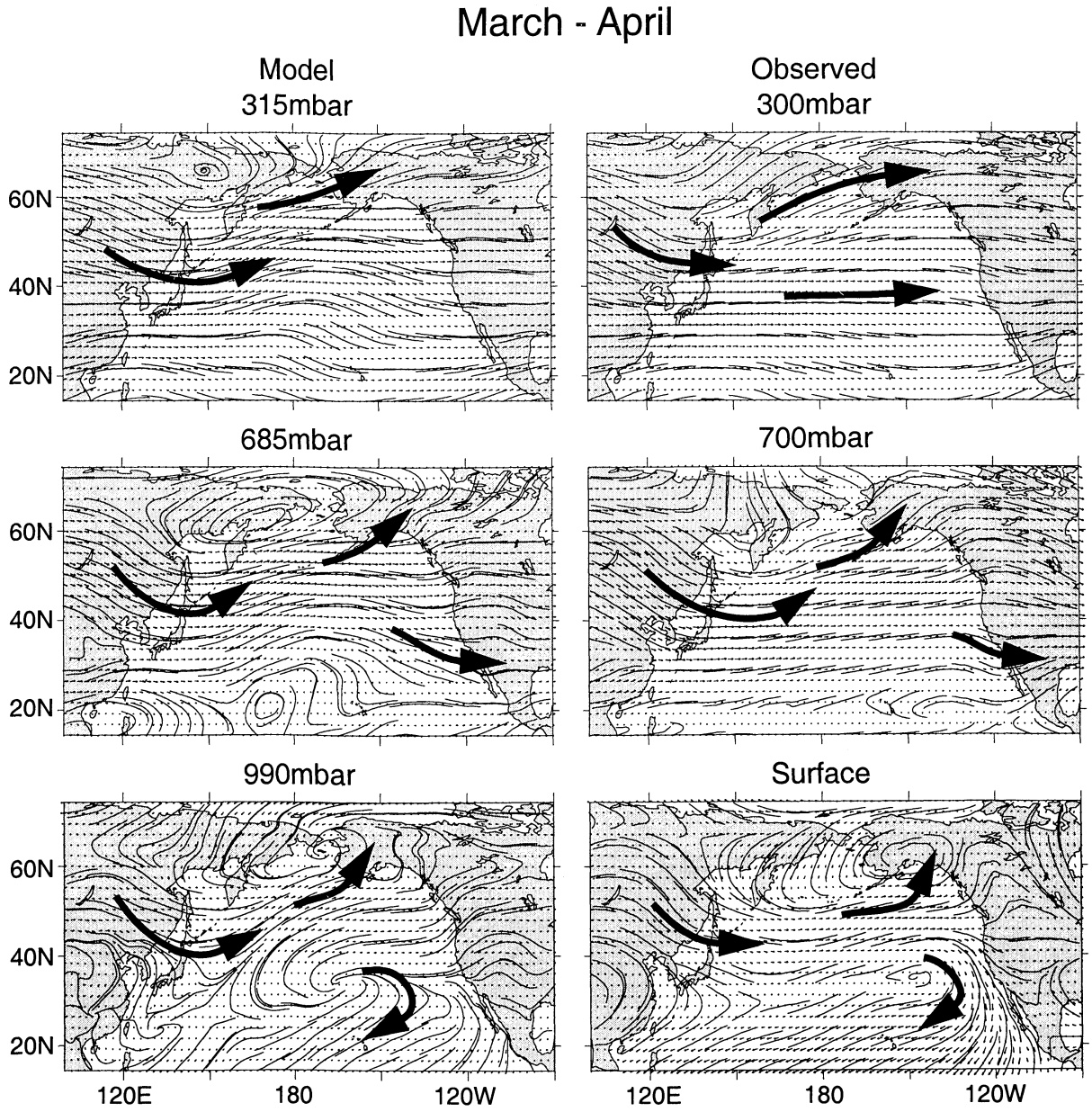

Figure 1. March-April mean streamlines over the North Pacific for the upper troposphere (~300 mbar), lower troposphere (~700 mbar), and surface. The model fields are constructed from the winds employed by the global chemistry transport model (GCTM) and the observed fields are from the analysis by *Oort* [1983].

tropospheric circulation over western Alaska, a midlatitude westerly flow across the North Pacific throughout the troposphere, and a boundary layer (BL) high-pressure circulation in the eastern subtropical Pacific producing the northeasterly tropospheric trade winds of the tropical Pacific.

However, in order to realistically simulate the observed episodic fluctuations in both relatively long-lived tracers such as CO and shorter-lived tracers such as O_3, the GCTM's transport must also contain realistic levels of synoptic variability. The GCTM's parent general circulation model (GCM) displays the appropriate eddy kinetic energy seasonal maxima in the regions of both the North Pacific and North Atlantic winter storm tracks [*Manabe et al.*, 1974]. In a spectral analysis of simulated N_2O time series, we showed that the dominant power in simulated tracer fluctuations in the midlatitude lower troposphere of the GCTM was in the synoptic range of 2 - 10 days [*Levy et al.*, 1982]. A detailed analysis of transport by a midlatitude storm over and off the coast of the eastern United States found that the GCTM realistically captured the main features of synoptic-scale transport (see Figure 5 and related discussion in the work by *Moxim et al.*, [1996]). Similar transport features are also captured by the GCTM over eastern Asia, as will be discussed in section 4.

2.2. CO Simulation

This work relies on the analysis of global simulations that have been described and extensively evaluated previously for CO [*Holloway et al.*, 2000] and O_3 [*Levy et al.*, 1997; *Klonecki and Levy*, 1997; *Yienger et al.*, 1999]. The GCTM simulation of CO is designed for 1990 conditions that include emissions from fossil fuel (300 Tg CO/yr), biomass burning (748 Tg CO/yr), biogenic hydrocarbon oxidation (683 Tg CO/yr) and CH_4 oxidation (758 Tg CO/yr). The only CO destruction pathway is OH oxidation based on precalculated monthly-mean 3-D OH fields [*Spivakovsky et al.*, 1990] that have been scaled by 1.15 to give a CH_3CCl_3 global lifetime of 4.8 years (see *Holloway et al.* [2000] for complete details of the CO simulation and its evaluation).

Seasonally averaged, 93% of the comparisons of GCTM simulations with surface observations from the global Climate Modeling and Diagnostics Laboratory (CMDL) flask network are within +-25% [*Holloway et al.*, 2000, Figure 7]. While the simulated monthly time series are generally in excellent agreement with the surface observations from Asia, the North Pacific, and North America, we do find an ~10 ppbv low bias in January through May at Midway Island, Cape Mears, Oregon,, and Wendover, Utah [see *Holloway et al.*, 2000, Figure 8]. While much of this bias could be removed by an increase in the global fossil fuel source from 300 to 400 Tg CO/yr, agreement would significantly worsen elsewhere. The ~20 ppbv January-May deficit at very high latitudes, which we believe results from excess downward transport of stratospheric air near the pole, may also influence the midlatitudes. This low bias does not significantly influence the synoptic-scale transport we are examining, as Plate 1 demonstrates. With the exception of the Asian and North American contribution analysis in Figure 5 and 6, which use an earlier CO simulation that employed the unscaled OH fields of *Spivakovsky et al.* [1990], this study employs the standard CO simulation. While the earlier simulation had ~7% more total CO, the relative contributions in Figure 5 and 6, which are transport controlled, do not differ significantly from the standard simulation.

2.3. O_3 Simulation

The ozone simulation has four components: irreversible stratospheric injection, parameterized pollution production in the continental boundary layer (BL), surface dry deposition, and CH_4-CO/acetone-H_2O-NO_x based chemistry throughout the background troposphere (see *Levy et al.* [1997], *Klonecki and Levy* [1997], *Yienger et al.* [1999] for details). The model's explicitly simulated stratospheric injection [*Levy et al.*, 1997] has been significantly improved by relaxing, with a 10-day lifetime, the GCTM's lower stratospheric ozone values to those simulated by the GFDL SKYHI GCM [*Hamilton et al.*, 1995; also L. Perliski, private communication, 1997]. The resulting global net stratospheric injection of ozone into the troposphere is 750 Tg O_3/yr.

The parameterized net production in the polluted continental boundary layer is derived from an empirical relationship between NO_x conversion and O_3 production based on midlatitude observations and theoretical studies and is employed when NO_x exceeds 200 pptv and isoprene exceeds 100 pptv. Both it and surface dry deposition are as described previously [*Kasibhatla et al.*, 1996; *Levy et al.*, 1997].

A CH_4-CO/acetone-H_2O-NO_x-O_3 photochemical box model is used to construct seven-parameter interpolation tables for 24-hour-averaged rates of ozone production and destruction in the background troposphere (NO_x < 200 parts per trillion by volume (pptv) and isoprene < 100 pptv). With CH_4 specified for each hemisphere, the eight parameters are tropospheric pressure, latitude, month, albedo, O_3, NO_y, CO, and H_2O (see *Klonecki and Levy* [1997] for details). The ozone production and destruction terms for every grid box in the background troposphere are then interpolated every time step from the tables using (1) the instantaneous ozone concentration from the current simulation; (2) 6-hour-sampled CO and NO_x concentrations from earlier simulations using the same meteorology; and (3) monthly averaged H_2O from observations [*Oort*, 1983; *Soden and Bretherton*, 1996]. Both the background O_3 chemical production and destruction and the pollution production respond to synoptic-scale fluctuations in O_3, CO and NO_x. While observed monthly-mean H_2O does not include synoptic-scale fluctuations, the dominant variations with height, latitude, and season are captured.

Although the O_3 simulation responds to fluctuations in the species important to O_3 chemistry, the same is not true for CO and NO_y, where monthly-mean zonally averaged chemical rates were used. This should not be a problem for CO, which has a chemical lifetime of weeks to months [see *Holloway et al.* 2000, Figure 2] and is not sensitive to day-to-day fluctuations in its chemical loss rate. While NO_x has a chemical lifetime of 1-3 days, OH and NO_x are positively correlated. This would tend to reduce the amplitude of the NO_x fluctuations, but should not significantly affect the mean response of the ozone chemistry, which is relatively linear over the expected range of NO_x [*Klonecki and Levy*, 1997]. We do not expect the lack of chemical feedbacks for NO_x and CO to affect the conclusions of this study.

In a comparison of the GCTM simulation with over 300 seasonal observations, both in the BL and at 500 mbar, from a global set of ozonesondes [e.g., *Logan*, 1999] and surface measurements [e.g., *Levy et al.*, 1997], ~90% of the cases are within +-25%, there is no global bias, and the seasonal amplitudes are realistic (see *Yienger et al.* [1999] and Plates 4a and 4b in this paper). However, the simulated means for many of the midlatitude sites are systematically ~10 ppbv high for January and February, although the respective standard deviations and means do generally overlap. In particular, the simulated 500-mbar mean at Sapporo, Japan, exceeds the observed mean by 15 ppbv in winter and 10 ppbv in spring.

2.4 Determination of Asian and North American Contributions to CO and O_3

To isolate pollution from Asia, we made three separate 2-year CO and NO_x simulations: one with full global emissions, one without surface emissions from Asia (defined to include South, Southeast, and East Asia), and one without surface emissions

from North and Central America. In the latter two cases, biogenic hydrocarbon oxidation and fossil fuel and biomass burning are considered surface sources of CO, and soil biogenic emissions and fossil fuel and biomass burning are considered surface sources of NO_x. The first year of the run is used to equilibrate the model, and the second year is used in analysis. We define the contribution of either Asia or North America to total CO (Asian CO and North American CO) as the difference between the full emission simulation and the respective simulations without the local emissions. Analogous pairs of O_3 simulations were run and differenced with the appropriate CO and NO_x fields to determine the impact of Asian emissions on total O_3, which we call "Asian O_3" (see *Levy et al.* [1999] for a detailed description of the NO_x sources and fields used in the 1990 simulations, and *Yienger et al.* [1999] for the methodology used to generate the future "2020" NO_x sources). Both 1990 and future NO_x emissions for South, Southeast, and East Asia are taken from *van Aardenne et al.* [1999].

The future projection, which is based on estimates of future growth in energy use and assumes that rising fossil fuel consumption will occur with no further emission controls, increases Asian NO_x emissions from 5.8 Tg N in 1990 to ~26 Tg by 2020. New evidence, however, indicates that controls are already being implemented on new energy developments in China and that 2020 emissions will likely not be so high (D. Streets, private communication, 1999). Therefore we consider our "2020" scenario a "worst-case scenario" and refer to it in section 5 as a fourfold increase in the 1990 Asian NO_x emissions of NO_x from fossil fuel combustion.

3. Episodic Asian CO Transport to North America

3.1. Cheeka Peak Observatory (CPO): Comparison to Observations

In Plate 1 we compare the GCTM's unfiltered total CO 940-mbar time series from a grid box just off the coast of CPO (see Figure 2) with the March-April 1997 [*Jaffe et al.*, 1999] and 1998 [*Jaffe et al.*, 2000] observations that have been filtered to remove obvious contamination by local pollution. The 940-mbar level was chosen to be at the altitude of CPO. Both of the GCTM simulations, the standard case in red and the old simulation with the unscaled *Spivakovsky et al.* [1990] OH in black, and the observations display similar amplitudes and frequencies of fluctuations. For this time period the standard simulation has a mean of 140 ppbv CO, while the 1997 observations are 151 ppbv and the 1998 observations are 170 ppbv. While both the 1997 observations and the simulation start to decrease in April, the 1998 observations remain high throughout, which accounts for the significantly higher mean. This 1998 behavior, although real, is the result of some unusual CO events which are now under investigation [*Jaffe et al.*, 2000].

For March and April of 1997, *Jaffe et al.* [1999] reported that 13% of all their isentropic trajectories crossed over East Asia compared to 16% of the fully 3-D trajectories in the GCTM. In most cases the GCTM parcels traveled from East Asia across the Pacific in 5-8 days, similar to the average of ~ 7 days and Figure 1 of *Jaffe at al.* [1999]. Interestingly, in both the model and

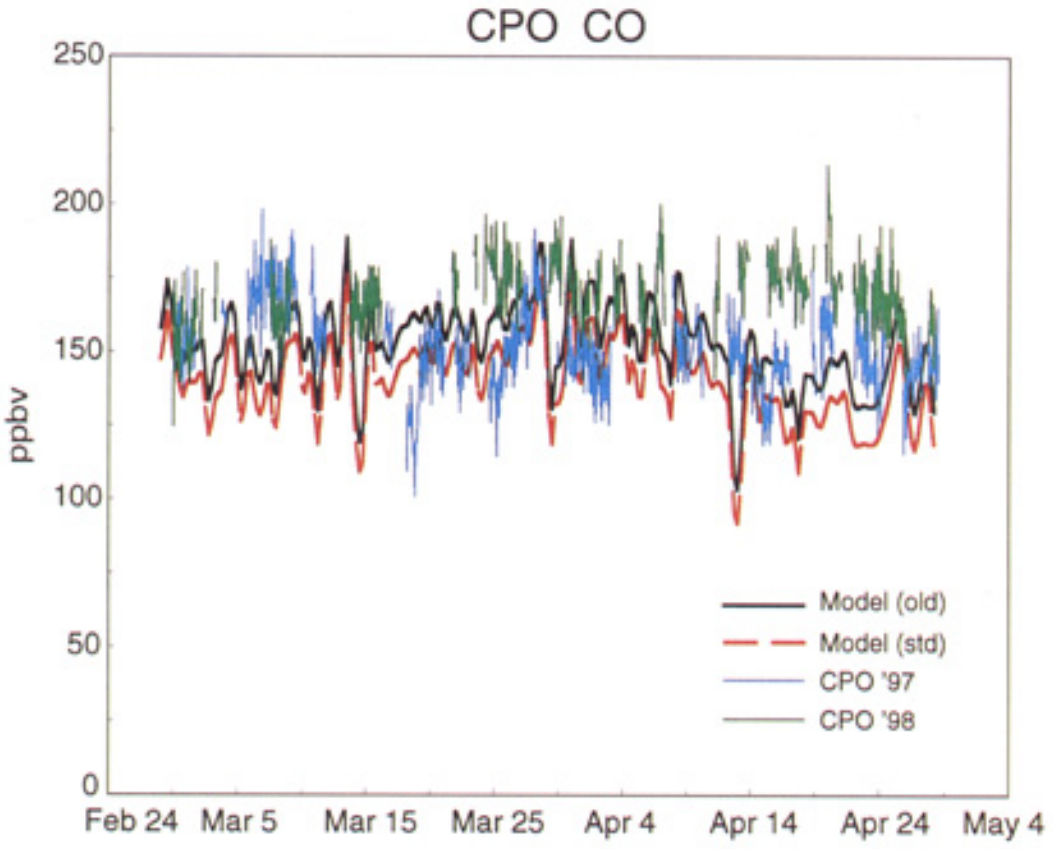

Plate 1. Comparison of the GCTM's 940-mbar time series of total CO with filtered observations from 1997 and 1998 from CPO. The red line is the standard CO simulation, and the black line is the earlier CO simulation with unscaled *Spivakovsky et al.* [1990] OH.

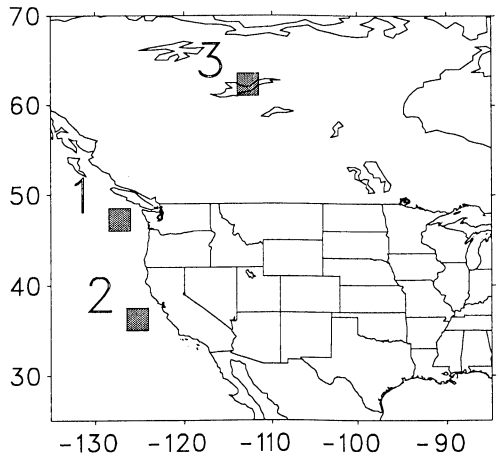

Figure 2. Locations of the three points analyzed in this study: (1) Cheeka Peak Observatory (CPO), (2) central California, and (3) north central Canada.

observations, not all "Asia trajectories" were associated with high levels of CO. In the GCTM we found that air descending over Japan behind troughs often arrived at CPO with relatively little Asian CO, while other GCTM events were associated with elevated Asian CO and raised ambient total CO by 20-30 ppb/d at CPO. Overall, we capture both the mean and the synoptic-scale fluctuations of total CO at CPO and the observed trajectory behavior [*Jaffe et al.*, 1999].

In Figure 3 we use the GCTM to explicitly consider the transport of Asian CO to CPO during winter and spring. Note that 35-40 ppbv of Asian CO is present as a background with a number of significant fluctuations and a few events of 60 ppbv or more. In order to estimate the number of events analogous in strength to those observed at CPO, we include a line at 55 ppbv that roughly defines the average amount of Asian CO we estimate to have been present during the major Asian events observed by *Jaffe et al.* [1999]. The 55-ppbv indicator was determined by adding the 18 ppbv mean difference between Asian and non-Asian trajectories (168 ppbv - 150 ppbv) observed by *Jaffe et al.* [1999] to the 35-40 ppbv background Asian CO in our simulation for a range of 53 - 58. This line isolates four major Asian pollution episodes and a number of lesser events. The number of significant Asian CO events, along with the fact that not all of them lead to significant total CO events at CPO, is consistent with the analysis and observations of *Jaffe et al.* [1999].

Interestingly, while there is a strong correlation between Asian and total CO, the three simulated peaks with the highest total CO (> 175 ppb) do not correspond to events with particularly high contributions from Asian CO, and represent three distinct 3-D trajectories. For the first peak (March 14), an "Asian trajectory" subsides into the BL over China and then travels across the North Pacific, but contains only the background level of Asian CO. The next two (March 29 and 31) both originate north of 60°N over far eastern Siberia and the Bering Sea, but the March 31 peak starts in the lower troposphere, subsides over eastern Siberia, and then travels across the North Pacific in the BL, while the March 29 peak starts in the BL and travels across the Bering Sea and down the coast of Alaska. Clearly, a variety of transport conditions can contribute to high-CO events at CPO, making an observation-based assignment of sources very complicated.

3.2. CO Variability Across North America

In Figure 4 we examine the relative frequency of Asian pollution events at three different grid points across NA (see Figure 2 for locations). The grid point off the coast of CPO has already been discussed. The second grid point represents background air arriving over central California, and the third point is in the high latitudes over central Canada. California was chosen because of obvious air quality concerns, while central Canada was chosen because this remote area will be used to evaluate the springtime evolution of ozone and related oxidants

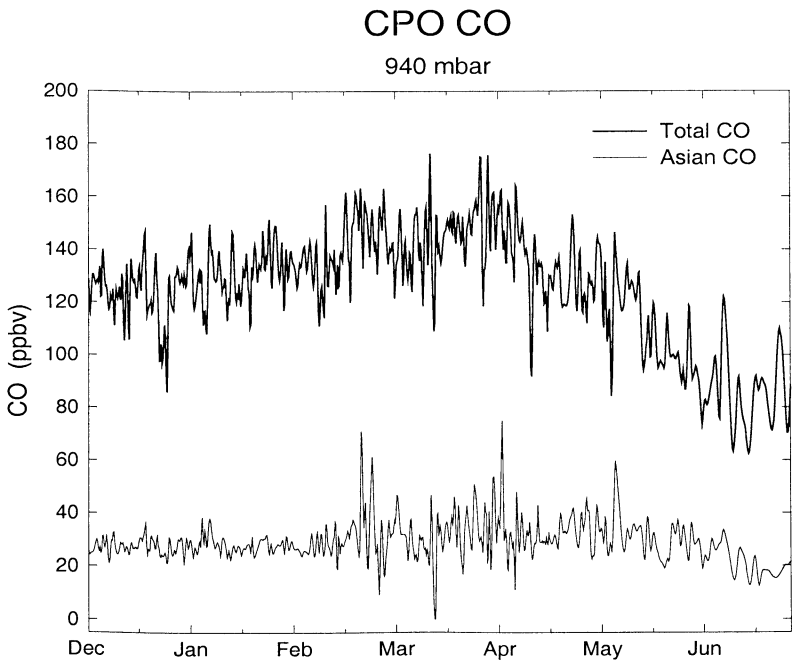

Figure 3. Time series at 6-hour intervals of simulated total CO and its Asian component (Asian CO) for the CPO grid box at 940 mbar.

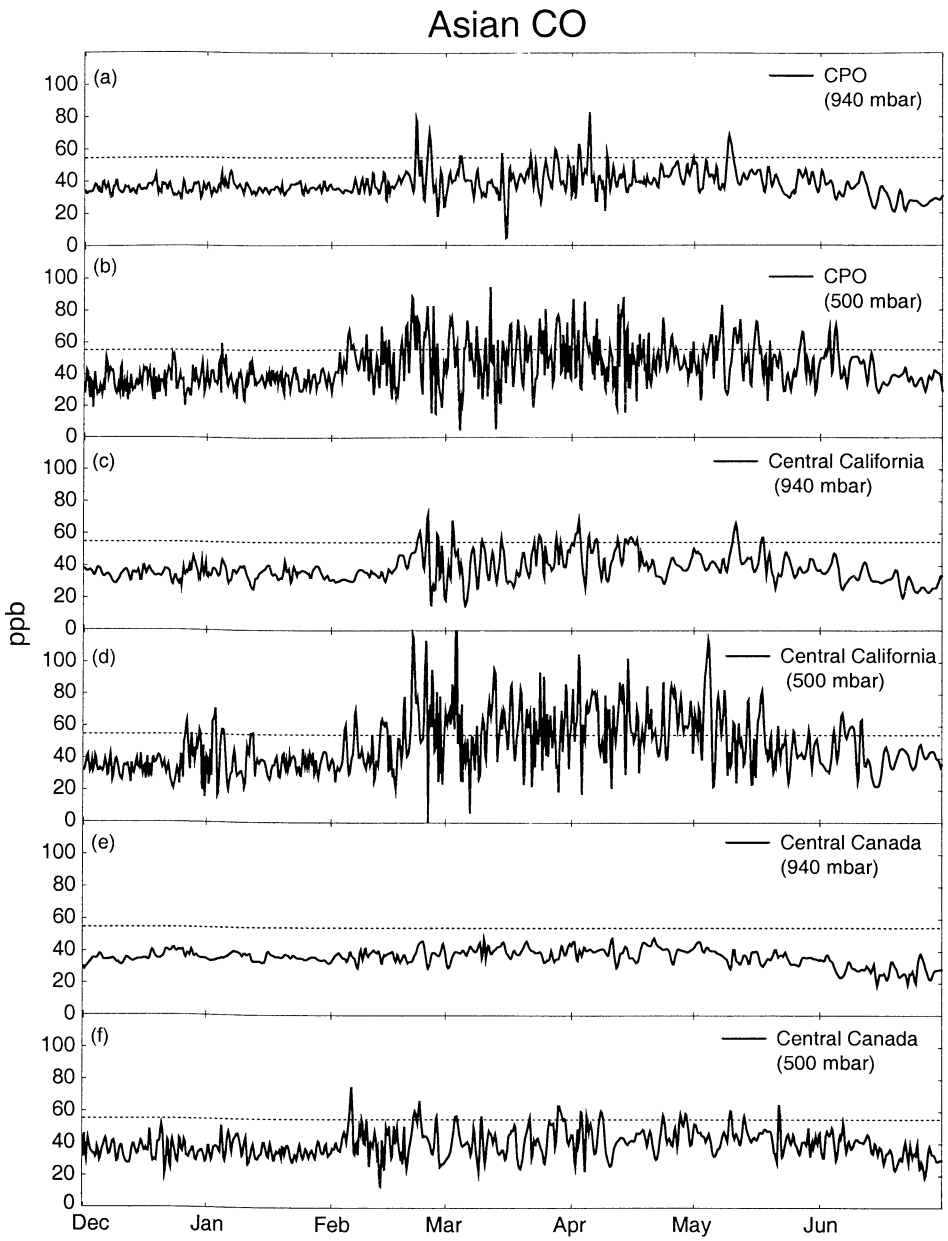

Figure 4. Time series at 6-hour intervals of Asian contribution to CO at all three locations in Figure 2 at both 940 mbar (boundary layer, BL) and 500 mbar (middle troposphere). Locations and pressure levels of the time series are labeled for each plot. The line at 55 ppbv represents an approximate baseline for major Asian CO events and our estimate of the approximate amount of Asian CO present in the Asian pollution parcels observed at CPO by *Jaffe et al.* [1999].

during the Tropospheric Ozone Production About the Spring Equinox (TOPSE) campaign. Free tropospheric measurements there will likely be influenced by Asia, but the nature and extent of this impact remain unknown. At each point we present results for both the boundary layer (940 mbar) and the middle troposphere (500 mbar).

Figures 4a-f reveal two major features in the frequency and magnitude of major Asian CO episodes: (1) Both frequency and magnitude increase sharply from the boundary layer to the middle troposphere at all sites, and (2) the high-latitude signal is dramatically smaller and less variable. Throughout the spring at CPO, major Asian CO events occur ~20% of the time at 500 mbar and only ~4% of the time in the BL. Trajectories from the GCTM reveal that flow from Asia is much more common aloft than in the BL. Moving southward to central California (Figure 4c) the Asian CO signal in the BL is similar to CPO though a little less noisy. Aloft at 500 mbar (Figure 4d) major Asian CO events occur even more frequently than at CPO and six exceed 100 ppb. Over central Canada, while the BL signal (Figure 4e) is muted and nearly always representative of the mean enhancement, there is still an obvious increase in the Asian signal at 500 mbar (Figure 4f), though the events are fewer and much smaller than they were for the midlatitude sites.

There is a growing awareness of the regional significance of annual burning in southern China and Indochina. Evidence for periodic enhancement of free tropospheric ozone over Hong Kong in spring due to biomass burning was recently reported by Liu et al. [1999]. During PEM West B, *Blake et al.* [1997]

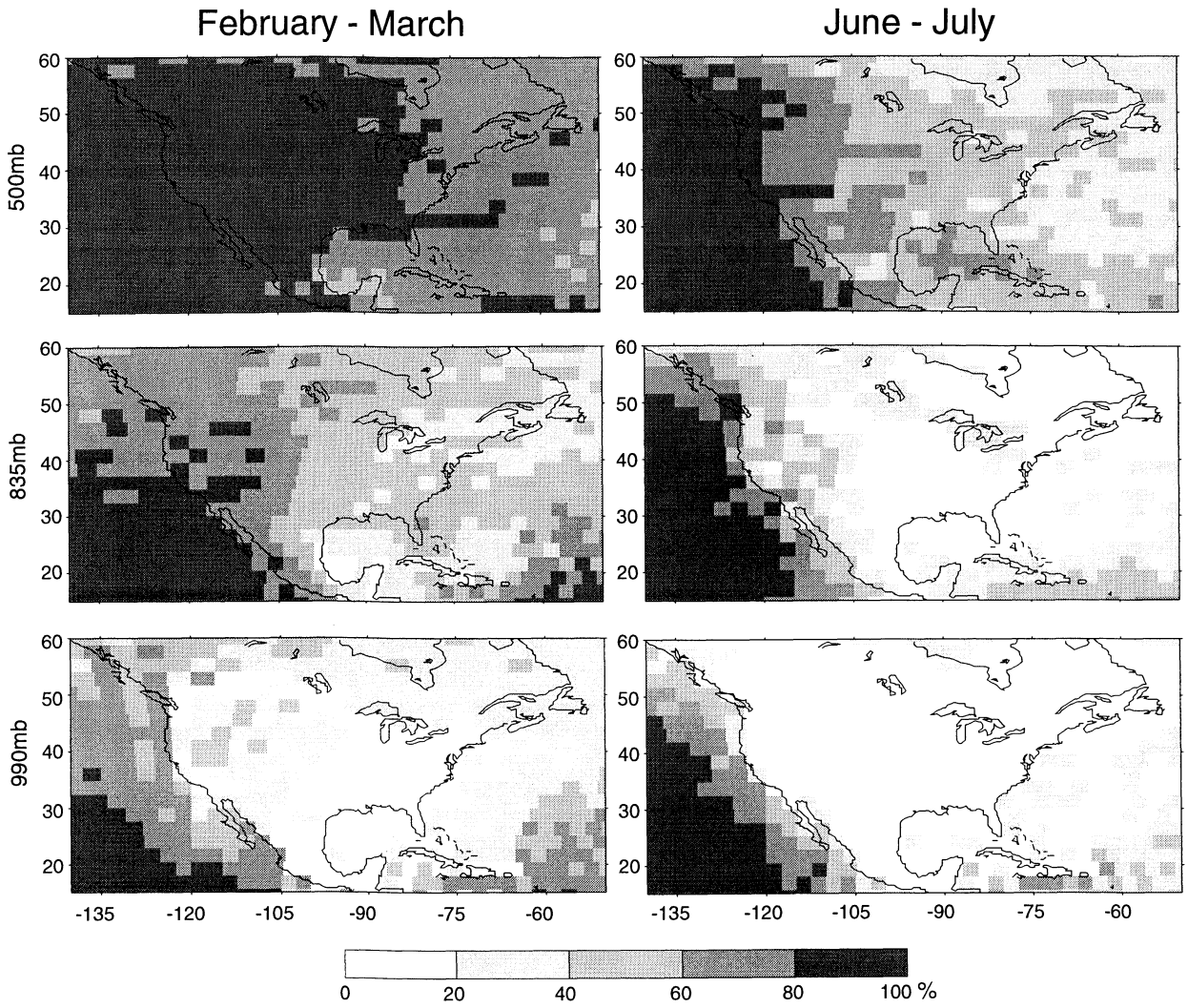

Figure 5. Plot showing the percent of the time that the Asian contribution to total CO exceeds the North American contribution. Analyses are for three levels (500 mbar, 835 mbar, and 990 mbar) and for two different periods (February-March and June-July).

reported that the outflow of combustion products observed below 25°N appeared to be from biomass burning, as opposed to farther north where the signal was distinctly urban. In addition, the satellite-derived Total Ozone Mapping Spectrometer (TOMS) aerosol index shows a consistent March-April maximum in southern China and Indochina that is likely to be caused by soot from biomass-burning fires [*Herman et al.*, 1997]. The trajectories for the largest Asian CO event (~80 ppbv) in early February at 500 mbar over central Canada and the four strongest (>100 ppbv) over California originate over southeastern Asia where spring biomass burning accounts for more than 50-70% of the local CO emissions [*Galanter et al.*, 2000]. This burning, which contributes 20%-30% of the total CO at 500 mbar over California, helps explain the high levels of Asian CO observed there.

3.3. Asian CO Versus North American CO

All the Asian CO episodes discussed up to this point have exceeded the North American contributions (recall that the NA contribution to total CO was computed analogously to Asian CO as the difference between a global simulation with and without North American, Mexican, and Caribbean surface CO sources). However, the importance of Asia to the overall chemical variability of the free troposphere is not limited to just the episodic peak events, nor to western NA. Much of the time, as shown in Figure 5, Asian CO exceeds NA CO in the free troposphere over much of North America. In February and March at 500 mbar, Asian CO is almost always greater than NA CO over most of the United States and southern Canada. In early spring, lack of convection generally shields the mid-troposphere from surface pollution. Lower down at 835 mbar, Asian CO still exceeds local CO 60-80% of the time over western NA and 40-60% of the time in the east. At the surface, local sources dominate with the exception of mountain grid boxes, which have small local sources and greater exposure to free tropospheric air. By June, slower transport, enhanced convection, and a shorter CO lifetime reduce the impact of Asian CO in the lower troposphere, although at 500 mbar Asian CO still dominates 40-80% of the time over NA.

The above percentages, while large, do not say whether the Asian source dominates during times of peak CO over NA or during low values resulting from either rapid ventilation or the absence of strong local sources. In order to put the percentages of Figure 5 into better perspective, we present in Figure 6

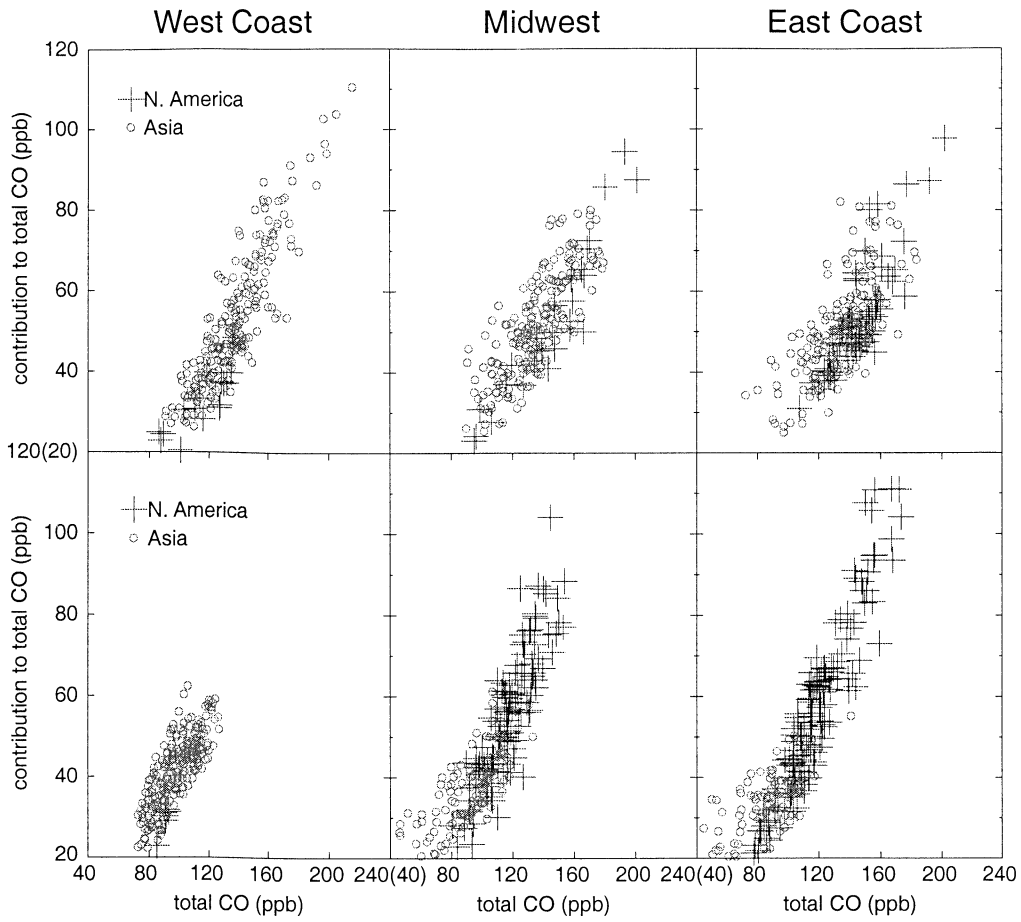

Figure 6. Scatter plots of simulated values of either Asian CO or North American (NA) CO versus total CO taken every 6 hours at 500 mbar for three grid boxes across the United States. If Asian CO exceeds NA CO, the Asian CO is plotted versus total CO as a circle. If the NA contribution is greater, it is plotted versus total CO as a plus. The top three plots are for February-March, while the bottom three are for June-July.

scatterplots of the contributions to total CO from Asia and North America versus total CO at 500 mbar for three grid boxes across NA: central California, the Midwest (Kansas), and the East Coast (Virginia). At each location we make two separate scatterplots for the periods of February-March and June-July to show the seasonal differences. A single point is plotted every 6 hours. If the Asian contribution exceeds the NA contribution, the Asian contribution is plotted against total CO as a circle, and if the reverse is true, the NA contribution is plotted against total CO as a plus. In this way, the regimes of CO when either source dominates are clear.

In February and March over California (500 mbar) the Asian contribution is clearly responsible for all the high CO values. During the relatively few periods when NA dominates, total CO is low. Moving eastward over the Midwest and East Coast, the frequency of synoptic-scale storms increases over the source regions, and the periods of high CO are due equally to NA and Asia. However, even over the East Coast, occasional contributions from Asia rival those from within North America itself. The model also shows that periods of high middle tropospheric CO over NA, regardless of origin, are as likely to occur over California as over the East Coast.

During June and July the situation at 500 mbar is quite different. Over California, Asia still dominates, although both total CO and the relative contribution from Asia are much smaller because of the shorter lifetime of CO and slower transport from Asia. Toward the east we attribute the highest values to NA CO lifted from the BL. Asia tends to still dominate about 50% of the time, but during the minima when air propagates all the way across NA without receiving a strong injection of CO from the BL. While there are still a number of moderate 50-60 ppb contributions from Asia that dominate during the middle-range CO events over the Midwest and East Coast, NA controls all the high CO levels.

4. Export From Asia

4.1. Synoptic-Scale Events

It is clear from Figure 1 that the springtime mean flow in the troposphere will tend to transport Asian emissions toward North America. When this flow is combined with CO's relatively long chemical lifetime, it is not surprising that there is a significant background level of Asian CO over NA. However, it is also clear from Plate 1 and Figures 3 and 4 that both total CO and its Asian component fluctuate a great deal with a synoptic-scale frequency of 2-10 days. An important mechanism for this episodic export of pollution from Asia is the development of low-pressure baroclinic systems over Asia that vent the BL and loft pollution into the free troposphere where it then may be carried rapidly across the North Pacific.

We found that the strongest Asian CO episodes over NA were often associated with amplifying troughs in the western Pacific

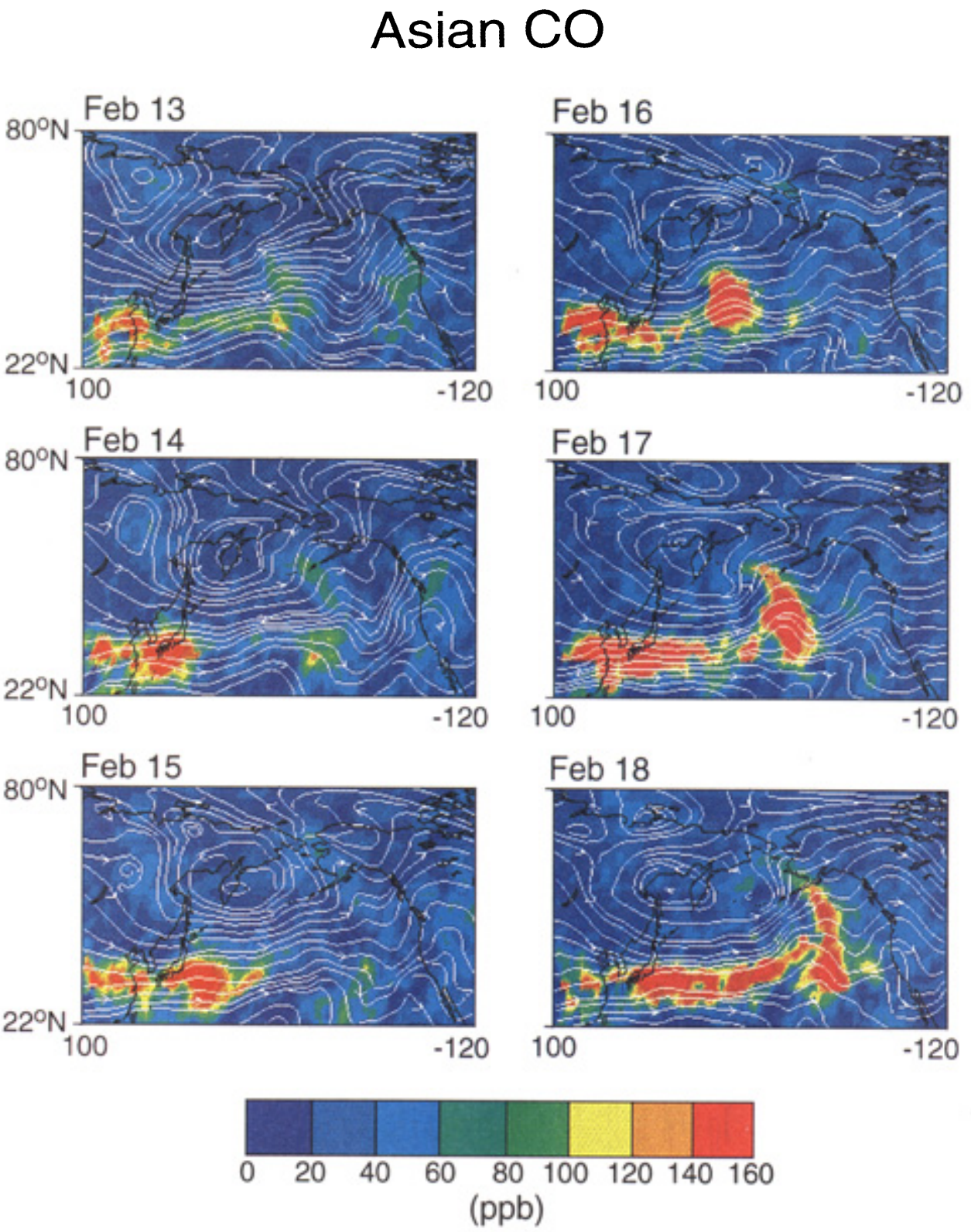

Plate 2. A six-plot 500-mbar daily sequence of Asian CO over the North pacific showing a trans-Pacific Asian CO transport event driven by cyclogenesis over Asia that propagated, with wave amplification in the middle troposphere, across the North Pacific. The white lines represent instantaneous streamlines. This sequence shows that parcels over Asia can, on occasion, advect fairly undiluted all the way across the Pacific Ocean. Movies of this and related transport events can be viewed at the following web site (http://www.cgrer.uiowa.edu/asiaimpact).

Ocean, an area of frequent cyclogenesis known as the Pacific storm track. The generalized nature of transport via baroclinic waves is well established [e.g., *Moxim et al.*, 1996; *Rood et al.*, 1997; *Stone et al.*, 1999]. These systems loft BL air into the free troposphere on the ridge side of the wave, and cause clean air to descend on the trough side of the wave. When cyclogenesis over Asia is followed by strong amplification in the storm track, accelerating westerly flows can move pollution from the continent to the central Pacific in a few days.

In Plate 2 we present a simulated 6-day sequence of Asian CO at 500 mbar during one such GCTM event in late February that produced the first high episodes at 500 mbar over California and CPO. On February 13 a surface low developed over China and lifted BL air into the free troposphere as it moved across China, Korea, and Japan (the remnants of two previous waves that vented Asian air can be seen on February 13 over the U.S. west coast and in the central Pacific). On February 15 it moved into the Pacific Ocean, intensified, and accelerated toward the west. By February 18 there is an Asian CO plume that features a maximum on the eastern side of the low pressure and a tail that extends back to Asia in the zonal flow.

This event so polluted the Pacific troposphere that episodic pockets of elevated CO arrived at locations all over the United States for a week. Notice that when the system reaches the Aleutian Islands, a plume extends virtually across the entire Pacific Ocean from East Asia. *Jaffe et al.* [1999] found such a pattern responsible for the strongest pollution episode observed at CPO and referred to it as a "conveyor-belt" in which flow is accelerated in a straight narrow band between the Aleutian Low and the Pacific High [e.g., *Jaffe et al.*, 1999, Figure 1]. The basic structure of this simulated event is also analogous to the April 1998 venting of the Asian BL that caused a large dust event over the western United States (R.B. Husar, http://capita.wustl.edu/Asia-FarEast). A sequence of NASA Goddard Space Flight Center satellite images shows that a Pacific storm entrains and evolves a dust plume (R.B. Husar, web sites, 1998) to a similar spatial and temporal scale as the CO plume shown in Plate 2.

4.2. Nature and Seasonality of Winter-Spring Asian Outflow

In winter the Asian CO signal shown in Figures 4a-f has low variability because cold surface temperatures over extratropical Asia create a stable low-level inversion that inhibits the venting of pollution out of the BL. Starting in late winter and early spring, however, convection into the middle troposphere increases as the Asian BL becomes less stable and cyclogenesis increases [*Chen et al.*, 1991]. By the end of May or early June, decreasing synoptic-scale storm activity, coupled with a weakening and northward movement of upper level westerlies, reduces the frequency and intensity of Asian outflow, as seen in Figures 4a-f.

During springtime, climatological differences between the middle and lower latitudes lead to different pathways for long-range transport out of Asia. From China, Korea, and Japan, which lie in prevailing westerly surface flow during spring, we found instances of both low- and high-altitude outflow, eventually leading to pollution episodes over NA. In general, lofting during

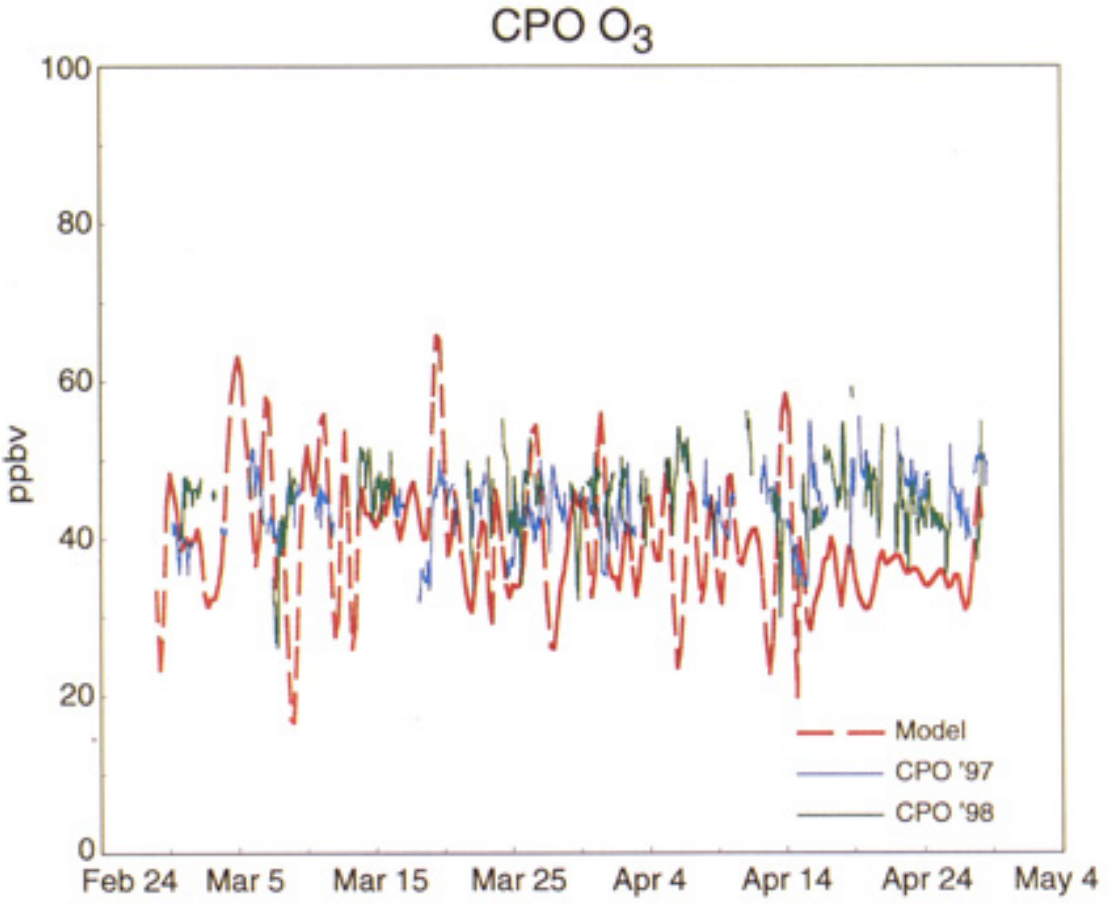

Plate 3. Comparison of the GCTM's 940-mbar time series of total O_3 with filtered observations from 1997 and 1998 from CPO.

storm passage and prevailing low-level flow between storms were both effective outflow mechanisms. On the other hand, most 3-D springtime trajectories that traveled back over southern China and Indochina did so in the middle troposphere, since long-range low-level outflow south of the storm track is inhibited by the prevailing northeasterly flow (see Figure 1). PEM West B analysis confirmed a sharp dropoff in the number of surface outflow events below 25°N as compared to the midlatitudes [*Talbot et al.*, 1997].

5. Episodic Impact of "Asian O_3" on Western NA

We would not expect the impact of Asia on O_3 across North America to be as pronounced as it is on CO because of ozone's shorter lifetime, the complex role of its background chemistry, the major contribution of local sources to local BL levels, and the major contributions to background ozone levels in the free troposphere from stratosphere-troposphere exchange (STE). Indeed, *Jaffe et al.* [1999] were unable to detect ozone enhancements during the episodes, attributed to Asian emissions, of springtime CO-aerosol-hydrocarbon pollution at CPO. This is consistent with the observed breakdown of the CO-O3 correlation far downwind of continents during spring [e.g., *Harris et al.*, 1998]. However, *Jacob et al.* [1999] predicted that by the year 2010, Asian emissions will raise mean surface ozone in California by ~6 ppb in May and ~3 ppb in July (relative to 1985), and they found that the impact will increase with altitude.

5.1. Cheeka Peak Observatory

In Plate 3 we compare our GCTM's 940-mbar O_3 time series from the ocean box upwind of CPO with the March-April 1997 [*Jaffe et al.*, 1999] and March-April 1998 [*Jaffe et al.*, 2000] observations from CPO, after the measurements contaminated by local pollution have been removed. As for CO, both the simulated time series and the observations show similar fluctuations. Unlike CO, the O_3 observations for the two years are quite similar in April, though like CO, they are both higher than the simulation. The model mean for the time period is 40 ppbv with a standard deviation (sd) of 8 ppbv, while for the observations the means are 44 and 45 ppbv with standard deviations of 5 and 4 ppbv for 1997 and 1998, respectively. While the simulated mean for the period, which has not been filtered, is within 10% of the observed means, it does show a number of fluctuations outside of the observed range and has twice the standard deviation.

We now examine the GCTM's two highest total O_3 peaks at CPO. The first peak (March 5) has a trajectory that originated over northern China at ~ 500 mbar, traveled across the North Pacific to Alaska at the same level, and then rapidly subsided while traveling down the coast of Alaska to CPO. The second (March 20) 3-D trajectory originated over China at 650 mbar, gradually subsided while crossing Korea, Japan, and the western North Pacific, and continued in the BL to CPO. Unlike the first peak, the trajectory for the second is extremely sensitive to its exact termination level at CPO. For a termination level of 900 mbar, the trajectory originates at 60°N and 660 mbar over Siberia, travels to the southeast, and subsides over Japan to 800 mbar and then heads straight over the North Pacific to CPO. While the two are quite similar from the central Pacific to CPO, they are quite different at the beginning, which suggests a complex meteorology over the western Pacific.

In Figure 7 we compare the GCTM's 940-mbar CPO time series for total O_3 and with the "Asian O_3" contribution for winter and spring. The obvious point is that the contribution of Asian emissions to O_3 at CPO, with a base of ~5 ppbv or 10-15%, is much smaller than it was for CO in Plate 1. It is also comparable to the 4 ppbv average found previously by *Berntsen et al.* [1999]. We also note that the total ozone values during the major Asian CO pollution episodes (denoted by solid circles in Figure 7) are not raised above background, although the contributions of "Asian O_3", itself, do maximize during the four Asian CO events.

Further complicating this picture is the fact that while the two largest O_3 events (>60 ppbv) have "Asian trajectories" according to the criteria of *Jaffe et al.* [1999], they experience only a background level of Asian influence (~5 ppbv) and are not associated with either major Asian CO events or large total CO events. Clearly, any attempt to attribute long-range impacts on the basis of local measurements and 5-10 day isentropic trajectory analysis at midlatitude is severely limited by the complexities of midlatitude synoptic meteorology, as well as the naturally large vertical and latitudinal gradients in O_3. The GCTM's day-to-day ozone variability over the North Pacific and the northwestern United States is strongly influenced by periodic subsidence events following the passage of cold fronts. Furthermore, O_3 injected from the stratosphere is highly correlated to ambient ozone in the spring and accounts for roughly 40% of the ozone arriving at CPO. In general, ozone arriving into the northwestern U.S. boundary layer has descended from a global-scale free tropospheric ozone reservoir that is not directly controllable by any one nation.

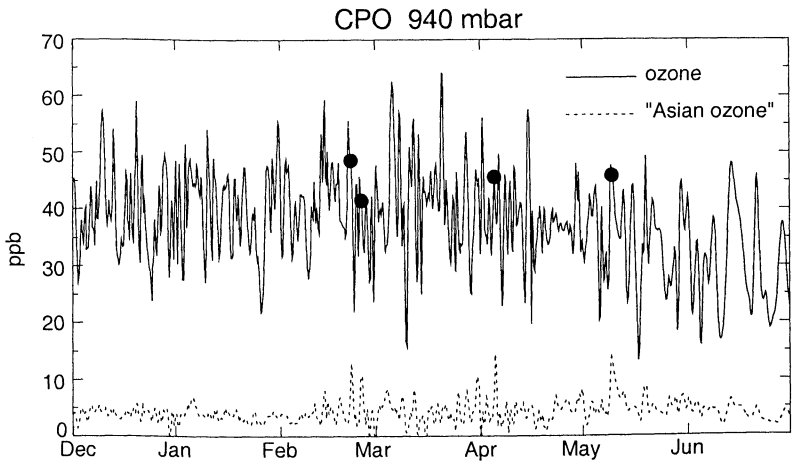

Figure 7. Time series in 6-hour intervals of ozone and its Asian component for the CPO grid box at 940 mbar. The four largest Asian CO events are marked on the ozone time series with solid circles.

5.2. Central California

Before examining the simulated impact of Asian emissions on California's O_3, we compare simulated 500-mbar and 940-mbar monthly-mean time series of total O_3 for January-June with 4 years of weekly ozonesonde observations from Trinidad Head, California (S. Oltmans, private communication, 2000) in the upper and lower plots, respectively, of Plate 4. Neither have been filtered for any possible local pollution, though the site, which is at the head of a peninsula in northern California jutting out into the Pacific Ocean, is normally expected to sample background air. The thin black line is sampled every 6 hours and captures the full variability in the GCTM simulation, while the thick black line has been sampled once a week, just as was done for the observations. Both the weekly sampled 500-mbar and 940-mbar simulated means and standard deviations (60 ppbv with a s.d. of 19 ppbv and 39 ppbv with a s.d. of 8 ppbv, respectively) are in excellent agreement with the observations (57 ppbv with a s.d. of 18 ppbv and 39 ppbv with a s.d. of 8 ppbv, respectively). However, the full simulation clearly has very strong synoptic-scale variability. This is driven by the arrival of baroclinic waves from the west every few days in the GCTM and is generally not captured in any of the weekly samples. There is no sign of the simulated synoptic variability in the December and January observations, though hints do appear in the other months. In a month-by-month analysis, we find excellent agreement between the GCTM and observations for all months at 940 mbar and all months excepting December and January at 500 mbar. For those two months the simulated standard deviations are much higher than observed, and the simulated January mean is 25% greater than observed.

In Figure 8 we present simulated 940-mbar and 500-mbar time series of "Asian O_3" in the grid box off the coast of central California for our 1990 emissions and for our 4x1990 Asian NO_x emissions ("2020") case. The January-June "Asian O_3" time series, as for Asian CO, are highly episodic, with the strongest O_3 events occurring later than for CO, probably due to a lag between the maximum Asian outflow and net photochemical ozone production. At 500 mbar with 1990 emission levels (Figure 8, upper plot), 4 events with greater than 20 ppb of "Asian O_3" occur in May and two each in March, April, and late February. Under the future scenario a few springtime events at 500 mbar approach 60 ppb, and most events greater than 40 ppb have shifted to April and May, periods which have more active photochemistry.

In the BL (Figure 8, lower plot), at 1990 emission levels a few Asian episodes exceed 10 ppb in March-May but drop to 5 ppb in June. Our 1990 "Asian O_3" contributions, driven by ~8 TgN/yr of Asian NO_x emissions, are similar in magnitude to the predicted increases from 1985 to 2010 of *Jacob et al.* [1999], which are driven by an increase of ~12 TgN/yr in NO_x emissions. While we found only a small Asian impact on current BL O_3, we predict that a four fold increase in Asian NO_x emissions, which is expected to occur sometime after 2020, will generate episodes of "Asian O_3" in the BL that reach 30-40 ppb in May and perhaps

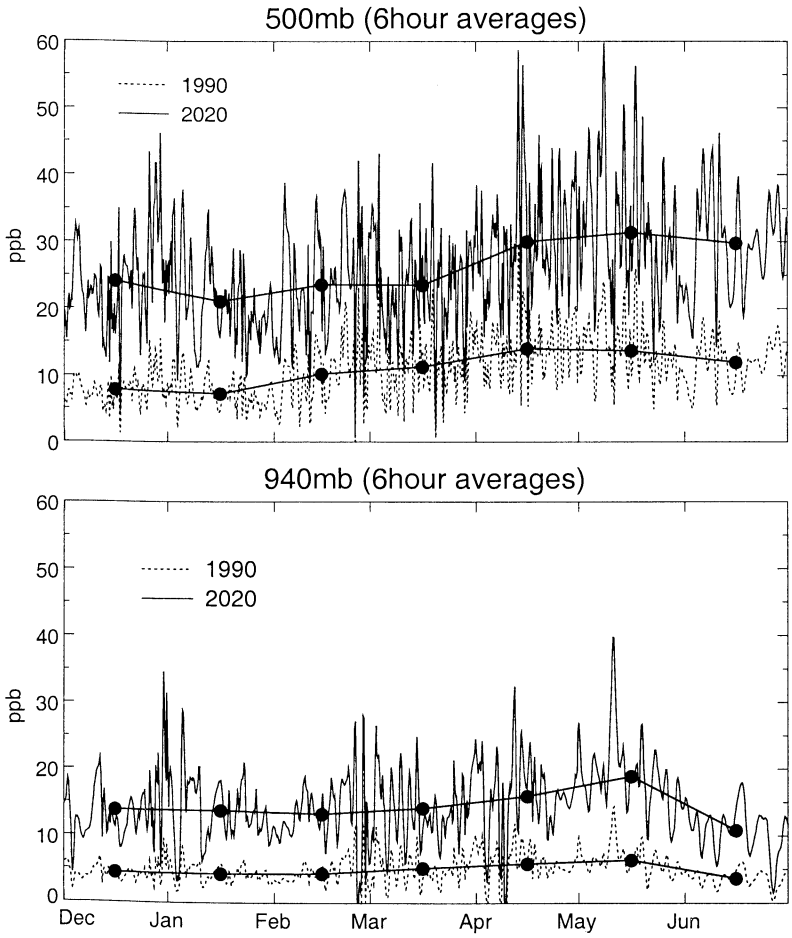

Figure 8. The Asian contribution to total ozone ("Asian O_3") offshore of central California at (top) 500 mbar and (bottom) 940 mbar. In both plots we present the time series for the 1990 emissions by a dotted line and the time series for the 4x1990 ("2020") Asian emission rates in black.

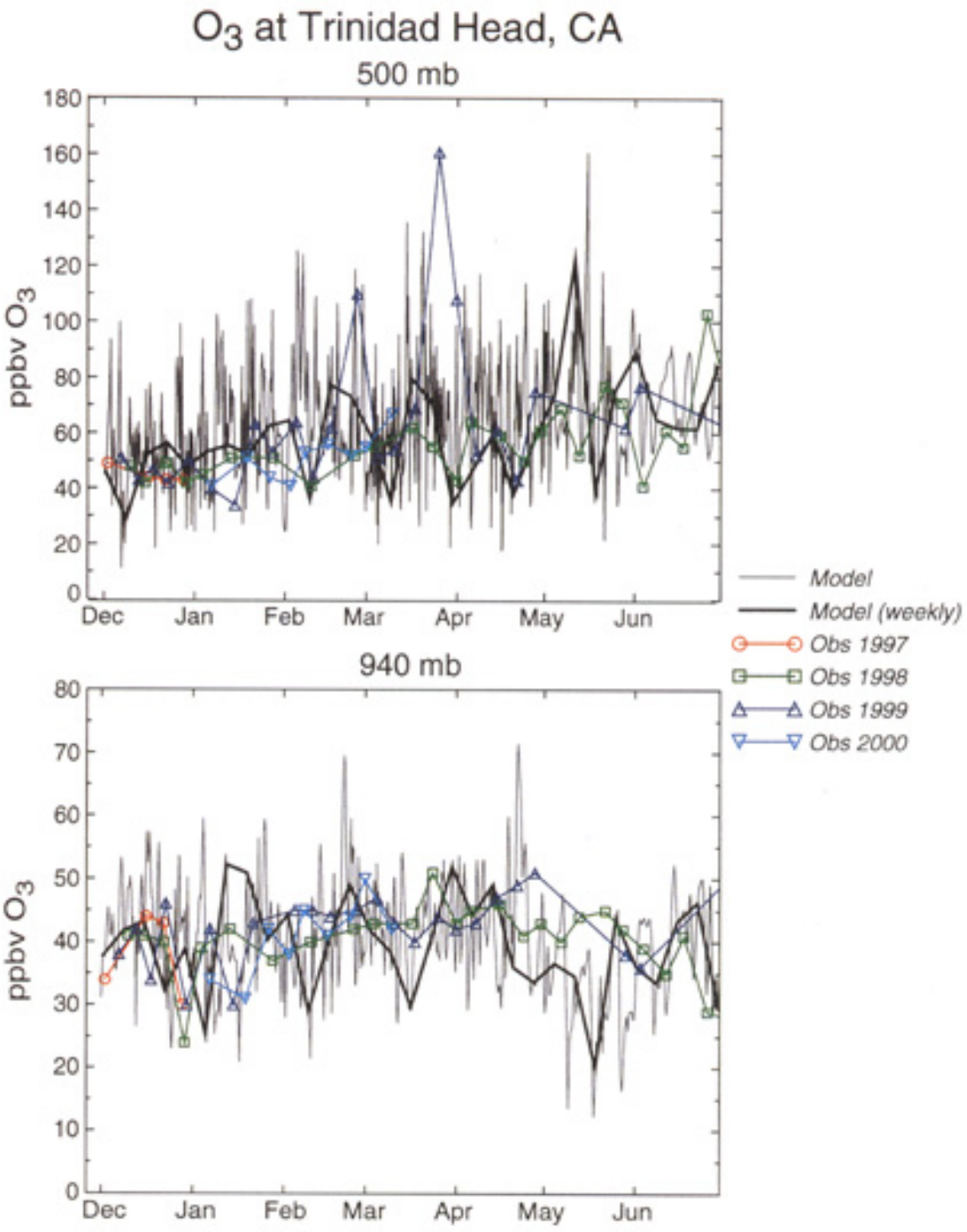

Plate 4. Comparison of the GCTM's 500-mbar and 940-mbar simulated O_3 time series with the ozonesonde observations from Trinidad Head, California for 1998-2000. For the GCTM the thin black line was sampled every 6 hours, and the thick black line was sampled once a week, while the observations were sampled weekly.

10-20 ppb in summer. In the future, such strong trans-Pacific events may well aggravate local pollution enough to generate violations of the current air quality standard for O_3. This is particularly true in higher altitude urban or suburban areas more exposed to free tropospheric air.

6. Conclusions

Our analysis of the episodic nature of trans-Pacific Asian contributions to North America CO and O_3 revealed the following:

1. With regard to the GFDL GCTM, its simulated total CO and total O_3 time series are in good agreement, both in the mean and in the magnitude and frequency of their fluctuations, with the surface observations of CO and O_3 at CPO and the ozonesonde observations at Trinidad Head California, and the GCTM's Asian trajectory analysis and number of significant Asian CO events simulated at CPO are consistent with the analysis of observations by *Jaffe et al.* [1999].

2. Using 55 ppbv of Asian CO as a baseline for major Asian pollution events from December - June, we found that their frequency and magnitude increased markedly with height, accounting for 20% of the total time series at 500 mbar over CPO and nearly 50% over central California, with some events exceeding 100 ppbv of Asian CO. Moving north over central Canada in the region of the TOPSE mission, we found that the overall signal variability decreased significantly. However, while there were no major Asian events in the BL, there were eight at 500 mbar.

3. In the springtime free troposphere over North America, Asian CO was found to exceed the contribution from North America most of the time in the west and up to three quarters of the time in the east. By summer, while Asian CO was still dominant over the western United States, it only dominated North American CO approximately one third of the time over the eastern United States, and in almost all cases only when total CO was low.

4. During winter and spring, Asian emissions made only a small contribution to western North American O_3 levels in the BL, while they played a larger, though not dominant, role at 500 mbar. For 1990 emissions, most boundary layer "Asian O_3" events in California were only in the 5-10 ppbv range during winter and spring and less in the summer.

5. While the GCTM simulated two 60+ ppbv total ozone events at CPO and their trajectories tracked back over the emission regions of Asia, neither Asian CO nor "Asian O_3" was significantly different from its normal background levels.

6. In a future emission scenario in which Asian NO_x emissions were increased by a factor of 4, episodes of late spring Asian ozone in the BL just off California were found to reach 40 ppb.

There are a number of implications of these results:

1. Given that the two largest total O_3 events simulated for CPO had "Asian trajectories" yet experienced only background levels of "Asian O_3" (~5 ppbv) and Asian CO (~40 ppbv), we can expect that attempts to attribute long-range air quality impacts on the basis of local measurements and 5-10 day isentropic back trajectories will be severely challenged by the complexities of midlatitude synoptic meteorology, as well as the naturally large vertical and latitudinal gradients in O_3. Many of the synoptic episodes of elevated total O3 and CO over the western United States appear to combine natural processes and pollution in a complex mixture of transport and chemistry.

2. Aerosol and chemical measurements in the free troposphere over North America will need to account for trans-Pacific transport when explaining synoptic-scale variability, particularly for those enigmatic high episodes that appear to have no local origin.

3. Regional-scale chemical models that rely on seasonal or monthly-averaged boundary conditions for either Pacific air or descending free tropospheric air over NA must consider the potential synoptic-scale consequences of such assumptions and may underestimate the variability in tracer time series when compared to observations.

4. While North American air quality does not now appear to be significantly affected by Asian emissions, it would appear that this may become a significant problem in the next few decades. This impact is much more likely to arise from synoptic-scale episodes than from a relatively steady increase in background O_3 levels.

Acknowledgments. This work was supported in part by NASA grants NAG5-3855 and NAGW-2428. We gratefully acknowledge Dan Jaffe for providing O_3 and CO data from CPO ahead of their publication and Sam Oltmans for providing ozonesonde observations from Trinidad Head, California prior to their publication. We also wish to acknowledge the helpful comments of an anonymous reviewer, and to explicitly thank Jennifer A. Logan for her insightful and extremely useful comments. We also wish to thank Jane Frank for editorial assistance and manuscript preparation.

References

Atlas, E. L., et. al., Partitioning and budget of NO_y species during the Mauna Loa Observatory Photochemistry Experiment, *J. Geophys. Res.*, 97, 10,449-10,462, 1992.

Berntsen, T. K., I. S. A. Isaksen, W. Wang, and X. Hang, Impacts of increased anthropogenic emissions in Asia on tropospheric ozone and climate, a global 3-D model study, *Tellus*, 48B, 13-32, 1996.

Berntsen, T. K., S. Karlsdottir, and D. Jaffe, Influence of Asian emissions on the composition of air reaching the north western United States, *Geophys. Res. Lett.*, 26, 2171-2174, 1999.

Blake, N. J., D. R. Blake, T. Chen, J. E. Collins, Jr., G. W. Sachse, B. E. Anderson, and F. S. Rowland, Distribution and seasonality of selected hydrocarbons and halocarbons over the western Pacific basin during PEM-West A and PEM-West B, *J. Geophys. Res.*, 102, 28,315-28,331, 1997.

Bodhaine, B. A., B. G. Mendonca, J. M. Harris, and J. M. Miller, Seasonal variations in aerosols and atmospheric transmission at Mauna Loa Observatory, *J. Geophys. Res.*, 86, 7395-7398, 1981.

Brasseur, G. P., D. A. Hauglustaine, and S. Walters, Chemical compounds in the remote Pacific troposphere: Comparison between MLOPEX measurements and chemical transport model calculations, *J. Geophys. Res.*, 101, 14,795-14,813, 1996.

Chen, S., Y. Kuo, P. Zhang, and Q. Bai, Synoptic climatology of cyclogenesis over East Asia, 1958-1987, *Mon. Weather Rev.*, 119, 1407-1418, 1991.

Duce, R. A., C. K. Unni, and B. J. Ray, Long-range atmospheric transport of soil dust from Asia to the tropical North Pacific: Temporal variability, *Science*, 209, 1522-1524, 1980.

Galanter M., H. Levy, II, and G. R. Carmichael, Impacts of biomass burning on tropospheric CO, NO_x, and O_3, *J. Geophys Res., 105*, 6633-6653, 2000.

Hamilton, K., R.J. Wilson, J.D. Mahlman, and L.J. Umscheid, Climatology of the SKYHI troposphere-stratosphere-mesosphere general circulation model, *J. Atmos. Sci., 52*, 5-43, 1995.

Harris, J. M., P. P. Tans, E. J. Dlugokencky, K. A. Masarie, P. M. Lang, S.Whittlestone, and L. P. Steele, Variations in atmospheric methane at Mauna Loa Observatory related to long range transport, *J. Geophys Res.*, 97, 6003-6010, 1992.

Harris, J. M., S. J. Oltmans, E. J. Dlugokencky, P. C. Novelli, B. J. Johnson, and T. Mefford, An investigation into the source of the springtime tropospheric ozone maximum at Mauna Loa Observatory, *Geophys. Res. Lett.*, 25, 1895-1898, 1998.

Herman, J. R., P. K. Bhartia, O. Torres, C. Hsu, C. Seftor, and E. Celarier, Global distribution of UV-absorbing aerosols from Nimbus 7/TOMS data, *J. Geophys. Res.*, 102, 16,911-16,922, 1997.

Holloway, T. A., H. Levy, II., and P. S. Kasibhatla, Global distribution of carbon monoxide, *J. Geophys. Res., 105*, 12,123-12,147, 2000.

Jacob, D. J., J. A. Logan, and P. P. Murti, Effect of rising Asian emissions on surface ozone in the United States, *Geophys. Res. Lett.*, 26, 2175-2178, 1999.

Jaffe, D., A. Mahura, J. Kelley, J. Atkins, P. C. Novelli, and J. T. Merrill, Impact of Asian emissions on the remote North Pacific atmosphere: Interpretation of CO data from Shemya, Guam, Midway, and Mauna Loa, *J. Geophys. Res.*, 102, 28,627-28,635, 1997.

Jaffe, D., et al., Transport of Asian air pollution to North America, *Geophys. Res. Lett.*, 26, 711-714, 1999.

Jaffe, D., T. Anderson, D. Covert, B. Trost, J. Danielson, W. Simpson, D. Blake, J. Harris, D. Streets, Observations of ozone and related species in the Northeast Pacific during the PHOBEA Campaigns: 1. Ground based observations at Cheeka Peak, *J. Geophys. Res.*, in press, 2000.

Kasibhatla, P. S., H. Levy, II, A. A. Klonecki, and W. L. Chameides, Three-dimensional view of the large-scale tropospheric ozone distribution over the North Atlantic Ocean during summer, *J. Geophys. Res.*, 101, 29,305-29,316, 1996.

Klonecki., A. A., and H. Levy, II, Tropospheric chemical ozone tendencies in CO-CH_4-NO_y-H_2O system: Their sensitivity to variations in environmental parameters and their application to a global chemistry transport model study, *J. Geophys. Res.*, 102, 21,221-21,237, 1997.

Kritz, M., The China Clipper-fast advective transport of radon rich air from the Asian boundary layer to the upper troposphere near California, *Tellus*, 42B, 46-61, 1990.

Levy, H., II, and W. J. Moxim, Influence of long-range transport of combustion emissions on the chemical variability of the background atmosphere, *Nature*, 338, 326-328, 1989.

Levy, H., II, J. D. Mahlman, and W. J. Moxim, Tropospheric N_2O variability, *J. Geophys. Res.*, 87, 3061-3080, 1982.

Levy, H., II, J. D. Mahlman, W. J. Moxim, and S. C. Liu, Tropospheric ozone: The role of transport, *J. Geophys. Res., 90*, 3753-3772, 1985.

Levy, H., II, P. S. Kasibhatla, W. J. Moxim, A. A. Klonecki, A. I. Hirsch, S., J. Oltmans, and W. L. Chameides, The human impact on global tropospheric ozone, *Geophys. Res. Lett.*, 24, 791-794, 1997.

Levy, H., II, W. J. Moxim, A. A. Klonecki, and P. S. Kasibhatla, Simulated tropospheric NO_y: Its evaluation, global distribution and individual source contributions, *J. Geophys. Res.*, 104, 26,279-26,306, 1999.

Liu, H., W. L. Change, S. J. Oltmans, L. Y. Chan, and J. M. Harris, On the springtime high ozone events in the lower troposphere from Southeast Asian biomass burning, *Atmos. Environ.*, 33, 2404-2410, 1999.

Logan, J., An analysis of ozonesonde data for the troposphere: Recommendations for testing 3-D models and development of a gridded climatology for tropospheric ozone, *J. Geophys. Res.*, 104, 16,115-16,149, 1999.

Mahlman, J. D., and W. J. Moxim, Tracer simulation using a global general circulation model: Results from a midlatitude instantaneous source experiment, *J. Atmos. Sci.*, 35, 1340 - 1374, 1978.

Manabe, S., D. G. Hahn, and J. L. Holloway, Jr., The seasonal variation of the tropical circulation as simulated by a global model of the atmosphere, *J. Atmos. Sci.*, 31, 43-83, 1974.

Merrill, J. T., R. Bleck, and L. Avila, Modelling atmospheric transport to the Marshall Islands, *J. Geophys. Res.*, 90, 12,927-12,936, 1985.

Merrill, J. T., M. Uematsu, and R. Bleck, Meteorological analysis of long-range transport of mineral aerosols over the North Pacific, *J. Geophys. Res.*, 94, 8584-8598, 1989.

Moxim, W. J., Simulated transport of NO_y to Hawaii during August: A synoptic study, *J. Geophys. Res.*, 95, 5717-5729, 1990

Moxim, W. J., H. Levy, II, and P. S. Kasibhatla, Simulated global tropospheric PAN: Its transport and impact on NO_y, *J. Geophys. Res.*, 101, 12,621-12,638, 1996.

Oort, A. H., Global atmospheric circulation statistics, 1958-1973, *NOAA Prof. Pap. 14*, 180 pp., U.S. Gov. Print. Off., Washington, D. C., 1983.

Prospero, J. M., Records of past continental climates in deep-sea sediments, *Nature*, 315, 279-280, 1985.

Prospero, J. M., and D.L. Savoie, Effects of continental sources on nitrate concentrations over the Pacific Ocean, *Nature*, 339, 687-689, 1989.

Ridley, B. A., et al., Aircraft measurements made during the spring maximum of ozone over Hawaii: Peroxides, CO, O_3, NO_y, condensation nuclei, selected hydrocarbons, halocarbons, and alkyl nitrates between 0.5 and 9 km altitude, *J. Geophys. Res.*, 102, 18,935-18,961, 1997.

Rood, R. B., A. R. Douglass, M. C. Cerniglia, and W. G. Read, Synoptic-scale mass exchange from the troposphere to the stratosphere, *J. Geophys. Res.*, 102, 23,467-23,485, 1997.

Soden, B. J., and F. P. Bretherton, Interpretation of TOVS water vapor radiances in terms of layer-average relative humidities: Method and climatology for the upper, middle, and lower troposphere, *J. Geophys. Res.*, 101, 9333-9343, 1996.

Spivakovsky, C. M., R. Yevich, J. A. Logan, S. C. Wofsy, M. B. McElroy, and M. J. Prather, Tropospheric OH in a three-dimensional chemical tracer model: as assessment based on observations of CH_3CCl_3, *J. Geophys. Res.*, 95, 18,441-18,471, 1990.

Stegmann, P. M., and N. W. Tindale, Global distribution of aerosols over the open ocean as derived from the coastal zone color scanner, *Global Biogeochemical Cycles*, 13, 383-397, 1999.

Stone, E. M., W. J. Randel, and J. L. Stanford, Transport of passive tracers in baroclinic wave life cycles, *J. Atmos. Sci.*, 56, 1364-1381, 1999.

Talbot, R. W., et al., Chemical characteristics of continental outflow from Asia to the troposphere over the western Pacific Ocean during February-March 1994: Results from PEM West-B, *J. Geophys. Res.*, 102, 28,255-28,274, 1997.

Uematsu, M., R.A. Duce, J. M. Prospero, L. Chen, J. T. Merrill, and R. L. McDonald, Transport of mineral aerosol from Asia over the North Pacific Ocean, *J. Geophys. Res.*, 88, 5343-5352, 1983.

van Aardenne, J.A., G.R. Carmichael, H. Levy, II, D. Streets, and L. Hordijk, Anthropogenic NO_x emissions in Asia in the period 1990 to 2020, *Atmos. Environ.*, 33, 633-646, 1999.

Wang, Y., D. J. Jacob, and J. A. Logan, Origin of tropospheric ozone and effects of nonmethane hydrocarbons, *J. Geophys. Res.*, 103, 10,757-10,768, 1998.

Xiao, H., G. R. Carmichael, J. Durchenwald, D. Thornton, and A. Bandy, Long-range transport of SO_x and dust in East Asia during the PEM B Experiment, *J. Geophys. Res.*, 102, 28,598-28,612, 1997.

Yienger, J. J., A. A. Klonecki, H. Levy, II, W. J. Moxim, and, G. R. Carmichael, An evaluation of chemistry's role in the winter-spring ozone maximum found in the northern midlatitude free troposphere, *J. Geophys. Res.*, 104, 3655-3667, 1999.

G.R. Carmichael, S.K. Guttikunda, M.J. Phadnis, and J.J. Yienger, Center for Global and Regional Environmental Research (CGRER), University of Iowa, Iowa City, IA 52242. (gcarmich@icaen.uiowa.edu)

M. Galanter, Department of Geosciences, Princeton University, Princeton, NJ 08544.

T.A. Holloway, Atmospheric and Oceanic Sciences Program, Princeton University, Princeton, NJ 08544.

H. Levy II and W.J. Moxim, Geophysical Fluid Dynamics Laboratory (GFDL)/NOAA, P.O Box 308, Princeton, NJ 08542. (gl@gfdl.gov)

(Received November 3, 1999; revised May 16, 2000;
accepted May 19, 2000.)